JOURNAL OF Applied Polymer SCIENCE

Special Issue: Bio-based Packaging

Guest Editors: José M. Lagarón, Amparo López-Rubio, and María José Fabra
Institute of Agrochemistry and Food Technology of the Spanish Council for Scientific Research

EDITORIAL

REVIEWS

RESEARCH ARTICLES

JOURNAL OF Applied Polymer SCIENCE

Special Issue: Bio-based Packaging

Guest Editors: José M. Lagarón, Amparo López-Rubio, and María José Fabra
Institute of Agrochemistry and Food Technology of the Spanish Council for Scientific Research

Impact of fermentation residues on the thermal, structural, and rheological properties of polyhydroxy(butyrate-*co*-valerate) produced from cheese whey and olive oil mill wastewater
L. Hilliou, D. Machado, C. S. S. Oliveira, A. R. Gouveia, M. A. M. Reis, S. Campanari, M. Villano and M. Majone, *J. Appl. Polym. Sci.* 2015, DOI: 10.1002/app.42818

Synergistic effect of lactic acid oligomers and laminar graphene sheets on the barrier properties of polylactide nanocomposites obtained by the in situ polymerization pre-incorporation method
J. Ambrosio-Martín, A. López-Rubio, M. J. Fabra, M. A. López-Manchado, A. Sorrentino, G. Gorrasi and J. M. Lagarón, *J. Appl. Polym. Sci.* 2015, DOI: 10.1002/app.42661

Antibacterial poly(lactic acid) (PLA) films grafted with electrospun PLA/allyl isothiocyanate fibers for food packaging
H. H. Kara, F. Xiao, M. Sarker, T. Z. Jin, A. M. M. Sousa, C.-K. Liu, P. M. Tomasula and L. Liu, *J. Appl. Polym. Sci.* 2015, DOI: 10.1002/app.42475

Poly(L-lactide)/ZnO nanocomposites as efficient UV-shielding coatings for packaging applications
E. Lizundia, L. Ruiz-Rubio, J. L. Vilas and L. M. León, *J. Appl. Polym. Sci.* 2015, DOI: 10.1002/app.42426

Effect of electron beam irradiation on the properties of polylactic acid/montmorillonite nanocomposites for food packaging applications
M. Salvatore, A. Marra, D. Duraccio, S. Shayanfar, S. D. Pillai, S. Cimmino and C. Silvestre, *J. Appl. Polym. Sci.* 2015, DOI: 10.1002/app.42219

Preparation and characterization of linear and star-shaped poly L-lactide blends
M. B. Khajeheian and A. Rosling, *J. Appl. Polym. Sci.* 2015, DOI: 10.1002/app.42231

Mechanical properties of biodegradable polylactide/poly(ether-block-amide)/thermoplastic starch blends: Effect of the crosslinking of starch
L. Zhou, G. Zhao and W. Jiang, *J. Appl. Polym. Sci.* 2015, DOI: 10.1002/app.42297

Interaction and quantification of thymol in active PLA-based materials containing natural fibers
I. S. M. A. Tawakkal, M. J. Cran and S. W. Bigger, *J. Appl. Polym. Sci.* 2015, DOI: 10.1002/app.42160

Graphene-modified poly(lactic acid) for packaging: Material formulation, processing, and performance
M. Barletta, M. Puopolo, V. Tagliaferri and S. Vesco, *J. Appl. Polym. Sci.* 2015, DOI: 10.1002/app.42252

Edible films based on chia flour: Development and characterization
M. Dick, C. H. Pagno, T. M. H. Costa, A. Gomaa, M. Subirade, A. De O. Rios and S. H. Flóres, *J. Appl. Polym. Sci.* 2015, DOI: 10.1002/app.42455

Influence of citric acid on the properties and stability of starch-polycaprolactone based films
R. Ortega-Toro, S. Collazo-Bigliardi, P. Talens and A. Chiralt, *J. Appl. Polym. Sci.* 2015, DOI: 10.1002/app.42220

Bionanocomposites based on polysaccharides and fibrous clays for packaging applications
A. C. S. Alcântara, M. Darder, P. Aranda, A. Ayral and E. Ruiz-Hitzky, *J. Appl. Polym. Sci.* 2015, DOI: 10.1002/app.42362

Hybrid carrageenan-based formulations for edible film preparation: Benchmarking with kappa carrageenan
F. D. S. Larotonda, M. D. Torres, M. P. Gonçalves, A. M. Sereno and L. Hilliou, *J. Appl. Polym. Sci.* 2015, DOI: 10.1002/app.42263

JOURNAL OF Applied Polymer SCIENCE

Special Issue: Bio-based Packaging

Guest Editors: José M. Lagarón, Amparo López-Rubio, and María José Fabra
Institute of Agrochemistry and Food Technology of the Spanish Council for Scientific Research

Structural and mechanical properties of clay nanocomposite foams based on cellulose for the food packaging industry
S. Ahmadzadeh, J. Keramat, A. Nasirpour, N. Hamdami, T. Behzad, L. Aranda, M. Vilasi and S. Desobry, *J. Appl. Polym. Sci.* 2015, DOI: 10.1002/app.42079

Mechanically strong nanocomposite films based on highly filled carboxymethyl cellulose with graphene oxide
M. El Achaby, N. El Miri, A. Snik, M. Zahouily, K. Abdelouahdi, A. Fihri, A. Barakat and A. Solhy, *J. Appl. Polym. Sci.* 2015, DOI: 10.1002/app.42356

Production and characterization of microfibrillated cellulose-reinforced thermoplastic starch composites
L. Lendvai, J. Karger-Kocsis, Á. Kmetty and S. X. Drakopoulos, *J. Appl. Polym. Sci.* 2015, DOI: 10.1002/app.42397

Development of bioplastics based on agricultural side-stream products: Film extrusion of *Crambe abyssinica*/wheat gluten blends for packaging purposes
H. Rasel, T. Johansson, M. Gällstedt, W. Newson, E. Johansson and M. Hedenqvist, *J. Appl. Polym. Sci.* 2015, DOI: 10.1002/app.42442

Influence of plasticizers on the mechanical and barrier properties of cast biopolymer films
V. Jost and C. Stramm, *J. Appl. Polym. Sci.* 2015, DOI: 10.1002/app.42513

The effect of oxidized ferulic acid on physicochemical properties of bitter vetch (*Vicia ervilia*) protein-based films
A. Arabestani, M. Kadivar, M. Shahedi, S. A. H. Goli and R. Porta, *J. Appl. Polym. Sci.* 2015, DOI: 10.1002/app.42894

Effect of hydrochloric acid on the properties of biodegradable packaging materials of carboxymethylcellulose/poly(vinyl alcohol) blends
M. D. H. Rashid, M. D. S. Rahaman, S. E. Kabir and M. A. Khan, *J. Appl. Polym. Sci.* 2015, DOI: 10.1002/app.42870

Journal of Applied Polymer Science

Impact of fermentation residues on the thermal, structural, and rheological properties of polyhydroxy(butyrate-*co*-valerate) produced from cheese whey and olive oil mill wastewater

Loic Hilliou,[1] Diogo Machado,[1] Catarina S. S. Oliveira,[2] Ana R. Gouveia,[2] Maria A. M. Reis,[2] Sabrina Campanari,[3] Marianna Villano,[3] Mauro Majone[3]

[1]Institute for Polymers and Composites, Institute for Nanostructures, Nanomodeling, and Nanofabrication, University of Minho, Campus de Azurém, 4800-058 Guimarães, Portugal

[2]UCIBIO, Rede de Química e Tecnologia, Departamento de Química, Faculdade de Ciências e Tecnologia, Universidade Nova de Lisboa, 2829-516 Caparica, Portugal

[3]Department of Chemistry, Sapienza University of Rome, Piazzale Aldo Moro 5, 00185 Rome, Italy

Correspondence to: L. Hilliou (E-mail: loic@dep.uminho.pt)

ABSTRACT: The effects of recovered residues on the characteristics of polyhydroxy(butyrate-*co*-valerate) (PHBV) produced from mixed microbial cultures (MMCs) fed with cheese whey, olive oil mill wastewater, or a synthetic mixture of acetic and propionic acid were investigated. The different types of MMC PHBVs were extracted and purified with different downstream routes; this enabled the recovery of polymers with different hydroxyvalerate contents and different residue types and levels, ranging from 0 to 11%. The results indicate overall that the recovery of residues together with the biopolymer brought benefits to the melt processability of these MMC PHBVs. Impurities triggered thermal degradation at smaller temperatures, promoted melting at lower temperatures, acted as thermal stabilizers, improved the melt viscosity, and enhanced the shear thinning. The degree of crystallinity of the aged samples was not affected by the impurities, but the crystallites size increased. MMC PHBVs recovered with residues containing more proteins showed better thermal stability, whereas MMC PHBVs containing more inorganic residues showed better melt viscoelastic properties. The results of this study show that impurities recovered together with the MMC PHBVs introduced changes to their thermal, semi-crystalline, and rheological properties; these changes, in some cases, were detrimental, but they were also potentially advantageous to the processing and conversion of these materials into products such as packages. © 2015 Wiley Periodicals, Inc. J. Appl. Polym. Sci. **2016**, *133*, 42818.

KEYWORDS: biodegradable; biopolymers and renewable polymers; rheology; thermal properties

Received 8 January 2015; accepted 7 August 2015

DOI: 10.1002/app.42818

INTRODUCTION

Polyhydroxyalkanoates (PHAs) are bacterial polyesters with a promising future for biobased packaging applications.[1–3] The main advantage of these biobased polymers is their compostability at room temperature. Thus, in contrast to other commercially available biodegradable polymers, such as poly(lactic acid), polycaprolactone, and petroleum-based biodegradable plastics, PHAs do not require the use of industrial composting facilities.[2] However, PHAs present several drawbacks that hamper their widespread industrial use, for example, in packaging.[4]

First, PHAs are very difficult to convert into packages with conventional plastic processing techniques. In addition to their low viscosity and melt strength, PHA thermal degradation occurs upon melting;[5] this depresses the final structural and mechanical properties of the plastic part or package. In this respect, polyhydroxy(butyrate-*co*-valerate) (PHBV) is a microbial copolyester showing lower melting temperatures (T_m's) than polyhydroxybutyrate. This contributes to a reduced thermal degradation during melt processing.[6]

Second, PHA, and to a lesser extent PHBV, is a brittle material, which shows slow crystallization kinetics followed by secondary crystallization. Slow crystallization is a strong drawback in applications such as injection molding, as it significantly extends the cycle time. The secondary crystallization is also an issue as packages will show aging and, thus, properties evolving with time. The brittleness virtually casts away PHA and PHBV from film packaging applications. Therefore, research efforts to improve PHBV transformation into packages has recently

Table I. Characteristics of the MMC PHAs

	CW 100%	CW 89%	OOMW 100%	SYNTH 100%	SYNTH 94%
HV content (mol %)	18	18	8–12	11.5	11.5
Purity (wt %)[a]	100	89.5 ± 2.7	100	100	94
Ash (wt %)		3 ± 1.6			NA
Water (wt %)		0.5			2.2
Proteins (wt %)		3.6 ± 0.3			0.45 ± 0.06
Sugars (wt %)		0.9 ± 0.4			0.15 ± 0.1
w (wt %)[b]	99	91	97	98	92
Inorganic (wt %)[c]	0.2	2.3	0.5	0.2	2.6
M_w (g/mol)	2.5×10^5	1.1×10^5	1.9×10^5	4×10^5	4×10^5
M_w/M_n	1.3	1.7	1.9	7	7

NA, not assessed because of the small amount of the sample available for analysis. Empty cells indicate that the amount of the corresponding impurity was below the limit of sensitivity of the technique used for its detection.
[a] Assessed with gas chromatography (see the Experimental section).
[b] Sample purity measured with TGA.
[c] Assessed with TGA.

focused on alternative processing routes to limit or eliminate thermal degradation, new formulations with natural fibers and other biodegradable plastics to improve the melt processability, and fermentation of new PHBV containing larger amounts of hydroxyvalerate (HV).[7–13]

Third, the market price of PHA and PHBV is still prohibitive compared to that of conventional plastics used for packaging. Strategies to reduce the production cost of PHA are flourishing. The use of mixed microbial cultures (MMCs) instead of pure cultures is now an established route for efficiently reducing production costs.[14,15] In addition, PHA recovery and purification add a large portion to the final product cost, and thus, efforts to improve PHA downstreaming are necessary.[16,17] PHA purification is important, as recovered residues lower the temperature for the onset of thermal degradation.[18,19] However, the effects of such residues on the processing and thermal and mechanical properties of PHA are still poorly documented.[20,21] Moreover, the effects of recovered PHA residue types and amounts on the rheological, thermal, and semicrystalline properties of PHA are not yet documented in the open literature.

The use of industrial food byproducts as substrates for the fermentation of PHA by MMC is a relatively new route that has been proposed to further lower the production cost of these microbial polyesters.[22] In particular, our research team recently reported the production of MMC PHBV with cheese whey (CW)[23] and olive oil mill wastewater (OOMW).[24] A multistage sequential process was designed to tailor the HV content in the microbial polyester while offering a high production rate.[23–25] Biopolyesters produced with the same process but with synthetic substrates (SYNTH) were recently characterized and tested for a packaging applications, where the casting of film-forming solutions was used.[13] This processing route involves the use of a solvent and subsequent filtration. Thus, MMC PHBVs are separated from the recovered residues, and this adds to the cost of packaging fabrication. The question arises as to whether the impurities associated with the recovered MMC PHBVs are detrimental to the material's thermochemical properties when purification during recovery is not complete. Less stringent PHBV recovery would enable the production of a more cost-effective biobased and biodegradable polymer, which would become an attractive alternative to the conventional fossil-oil-based plastics used in applications such as packaging.

According to earlier results,[13] a set of MMC PHBV samples with tailored HV contents, namely, 8–12 and 18 mol %, were produced with OOMW and CW, respectively. The characteristics of the starting materials, namely, OOMW and CW, have been given elsewhere,[23,24] together with details on the production of the corresponding MMC PHBVs. The targeted HV contents were selected as they gave biopolyesters with low T_m's, intermediate glass-transition temperatures (T_g's), and mechanical properties that were acceptable for packaging applications. In addition to CW and OOMW, SYNTHs were also used to produce the selected PHBVs to vary the type of recovered PHA residues.[25] In this contribution, we focus on the effect of recovered PHA residues on MMC PHBV properties that are relevant to melt processing. The MMC PHBVs produced in previous studies[23–25] were submitted to different downstreaming routes in this study; this allowed the delivery of a set of MMC PHBVs with different amounts and types of recovered PHA residues. The thermal, structural, and rheological properties of these MMC PHBVs were studied to assess the effects of the recovered PHA residues on properties that were relevant for the conversion of polymers into packages.

EXPERIMENTAL

Three MMC PHBVs were produced with nearly similar purities but with different HV contents and molecular mass distributions. These MMC PHBVs were submitted to similar downstream processes, but different accumulation methods and feeding substrates were used. Comparisons between these three biopolyesters, namely, CW 100%, OOMW 100%, and SYNTH 100%, allowed us to assess the combined effects of the molecular masses, HV contents, and distribution in the polymer chain

on the MMC PHBV characteristics. In addition, two sets of MMC PHBVs were produced both with a base recovery providing about 90 ± 2% purity; this was followed by a secondary purification to reach a sample purity of nearly 100%. Therefore, this study provided an experimental design with replicates of low and high purity, whereby the effects of the residues (of similar orders of magnitude but with different compositions, as shown in Table I) on the PHBV characteristics could be discussed. In this section, we start with a brief description of the production of the MMC PHBVs, as detailed reports on the polymer production and characteristics are given elsewhere.[23–25] Then, the purification of the MMC PHBVs is detailed along with all of the experimental techniques used for the characterization of all of the polymers.

Production of the MMC PHBVs

The PHBV from CW was produced in a 20-L feed-batch reactor by the feeding of fermented CW to a selected PHA-accumulating MMC. The fermented CW was obtained through the acidogenic fermentation of a suspension of CW powder in a 10-L continuous membrane bioreactor (AnMBR) operated at temperatures between 30 and 37°C, at a pH of 5–6, and with hydraulic and sludge retention times of 1 and 4 days, respectively. The PHA-accumulating MMC was selected in a 100-L sequencing batch reactor (SBR) fed with a synthetic volatile fatty acid (VFA) mixture (acetate, propionate, butyrate, and valerate) supplemented with nutrients (NH_4Cl and KH_2PO_4) at an organic loading rate (OLR) of 50 millimoles of carbon atoms (Cmmol) L^{-1} day^{-1}, a 1-day hydraulic retention time, and a 4-day sludge retention time. The PHA accumulation reactor was inoculated with the selected PHA-accumulating MMC and fed pulse-wise with the fermented CW controlled by the dissolved oxygen response. An average PHA cell content of 38 wt % was reached. At the end of the PHA accumulation assays, the microbial activity was rapidly quenched by the application of an extremely low pH (between 2 and 3) through the addition of 4*M* HCl. The PHA-saturated biomass was concentrated twofold in volume by the settling and decanting of the supernatant, and an NaClO (5% Cl) solution was added at a ratio of 1 g of NaClO/g of cell dry weight. The mixture was stirred at room temperature for 3 h to degrade the non-PHA cellular material. The polymer was then recovered by centrifugation (for 15 min at 6500 rpm) and washed four times with distilled water. The final product was obtained after a two-step drying process: first, most of the water was evaporated at 40°C for 2 days, and then, the material was completely dried at 70°C for about 5 h. The dried polymer was lightly crushed into a powder and kept in a desiccator in the dark. This polymer was labeled CW 89%.

The PHBV from OOMW was produced in a laboratory-scale PHA-accumulating reactor (0.70-L working volume) with the MMC selected in an SBR (1-L working volume) fed with a synthetic mixture of VFAs in a balanced mineral medium containing ammonium and phosphate salts as N and P sources.[25] Specifically, the SBR feed consisted of acetic acid (0.87 moles of carbon atoms (Cmol)/Cmol of VFA) and propionic acid (0.13 Cmol/Cmol of VFA) at an overall OLR of 260 Cmmol L^{-1} day^{-1}, and the hydraulic and sludge retention times were set at 1 day. The length of each SBR cycle was 6 h; this accounted for four cycles per day. The MMC discharged from the SBR was sent to the accumulation reactor, pulse-fed with pretreated OOMW (i.e., 50 mL of OOMW was added to the reactor every 20 min for 3 h). No nutrients were added during the accumulation assays. The OOMW pretreatment mainly consisted of an acidogenic fermentation stage, in which we aimed to increase the VFA content of the wastewater. Before it was used for PHA production, the pretreated OOMW was subjected to a solid–liquid separation stage by centrifugation (for 20 min at 8000 rpm), and the liquid fraction was fed into the accumulation reactor. After the accumulation assays, the mixed liquor of the reactor was centrifuged (for 20 min at 8000 rpm) to separate the PHA-rich cells (the pellet) from the supernatant. To recover the polymer, the pellet was treated with an NaClO (5% Cl_2) solution and kept under continuous mixing for several hours at room temperature. The mixture was then centrifuged (for 15 min at 8000 rpm), and the pellet was lyophilized for around 96 h. Finally, the lyophilized sample was dissolved in chloroform at 60°C for about 1 day and then precipitated drop by drop in an iced methanol solution kept under stirring. Finally, the precipitate was filtered and the solid fraction was dried at 60°C overnight. Throughout the article, this polymer is referred to as OOMW 100%.

As for the polymer labeled SYNTH 94%, it was produced with the MMC selected in an SBR fed with a synthetic mixture of acetic and propionic acid at an OLR of 260 Cmmol L^{-1} day^{-1}, as previously described.[25] PHA accumulation with the selected MMC was performed in a laboratory-scale reactor (with a 0.30-L working volume) fed with a mixture of acetic and propionic acids at a very high OLR (890 Cmmol L^{-1} day^{-1}) and operated in batch mode with each batch lasting 6 h; this accounted for four batches per day. After 6 h of accumulation, the entire liquid volume of the reactor was sent to the extraction reactor to be mixed with the digestion solution (NaClO with 5% Cl_2) for several hours at room temperature; it was subsequently centrifuged (for 30 min at 8600 rpm) and lyophilized for around 96 h.

With the aim of obtaining polymers with a minimal amount of residues, we mixed 6 wt % nonpurified polymer (samples CW 89% and SYNTH 94%) in chloroform at 40°C for 12 h and at room temperature for 24 h to ensure the maximum solvation of PHBV. The mixture was then filtered (0.45 μm) and precipitated in 2.5 volumes of iced methanol. The precipitate was then filtered, washed with methanol, and eventually dried at 60°C in a vacuum oven overnight. With this purification, two samples were recovered, namely, CW 100% and SYNTH 100%.

The purity (i.e., amount in grams of produced PHA with respect to the total amount of sample) and composition (i.e., the HV content in the produced polymer) of the MMC PHBV samples were determined with gas chromatography (PerkinElmer 8410 gas chromatographer/flame ionization detector), as described elsewhere.[25] In addition, the impurities in samples SYNTH 94% and CW 89% were characterized as follows. The water and ash contents were determined by the sample weights after 24 h at 100°C and 2 h at 550°C, respectively. Elemental analysis was performed in an inductively coupled plasma-

Table II. T_d (Measured with TGA) and T_g, T_c, T_{m1}, T_{m2}, and χ_c (Measured during the DSC Heating Run Performed after Cooling from the Melt)

Sample	T_d (°C)	T_g (°C)	T_c (°C)	T_{m1} (°C)	T_{m2} (°C)	χ_c (%)
CW 100%	300	1	62	147	163	28
CW 89%	283	−3	82	126	144	25
OOMW 100%	305	0	81	133	150	20
SYNTH 100%	302	2	76	140	158	22
SYNTH 94%	297	1	82	133	151	18

The experimental error for the transition temperatures was 1°C with DSC and 2°C with TGA.

atomic emission spectrometer (ICP-Ultima ICP, Horiba Jobin-Yvon, France). The protein content was determined spectrophotometrically at 750 nm by the alkaline copper method, as described elsewhere.[26] Bovine serum albumin was used as a protein standard for determining the calibration curve (0–200 mg/L). The total sugar content was determined by the measurement of the absorbance at 490 nm of the samples treated with phenol (5% w/w) and concentrated sulfuric acid.[27] Sucrose was used to determine the standard curve (0–100 mg/L).

The average molecular weights of the samples CW 100% and CW 89% were determined with a size exclusion chromatography apparatus (Waters) according to a protocol described elsewhere.[28] The molecular mass distribution of samples OOMW 100%, SYNTH 100%, and SYNTH 94% were determined with gel permeation chromatography according to a protocol reported elsewhere.[25]

IR Spectroscopy

Fourier transform infrared (FTIR) spectroscopy was performed on powder samples (dried overnight in an oven at 60°C) at room temperature with a diffuse reflectance sampling accessory [diffuse reflectance infrared Fourier transform (DRIFT)] of an FTIR spectrometer (Spectrum 100, PerkinElmer, Ltd.) by the averaging of 16 scans with a resolution of 4 cm^{-1} from 500 to 4000 cm^{-1}.

Characterization of the Thermal Properties

The thermal stability of the samples was measured by means of thermogravimetric analysis (TGA) carried out with a TA Q500 instrument (TA Instruments) with sweeping temperatures between 30 and 600°C at a heating rate of 20°C/min under an air atmosphere and typically with 10–20 mg samples. Differential scanning calorimetry (DSC) was carried out on powder samples (typically, 4–8 mg, dried overnight at 60°C) with a DSC instrument from Netzsch at a heating rate of 10°C/min from −30 to 180°C (run I); this was followed by cooling to −30°C at −10°C/min and, finally, reheating at 10°C/min up to 180°C (run II), always under an air atmosphere. The cooling DSC curves were featureless for all of the samples. The T_g's, crystallization temperatures (T_c's), and T_m's (T_{m1} and T_{m2}) were determined from run II. The crystallinity degrees (χ_c's) were computed with a reported melting enthalpy for a 100% crystalline PHB[29] (ΔH_0) of 146 J/g and the following equation:

$$\chi_C = \frac{100 \times \Delta H}{\Delta H_0 \times w} \quad (1)$$

where ΔH is the melting enthalpy measured during run II and w is the purity of the sample determined from the TGA experiments (see later). After 1 week of aging of the samples in DSC pans, a third heating similar to run I was performed to measure the T_g's (T_{g1} and T_{g2}) and T_m's (T_{m3} and T_{m4}).

Wide-Angle X-ray Diffraction (WAXD)

The structure of the samples rimmed from rheological testing (see later) was assessed by WAXD with a Bruker D8 Discover diffractometer (λ source = 0.154 nm). The samples were aged for 1 month at room temperature. The scanning range was 2θ = 5–35° with 0.04° steps. The WAXD patterns were deconvoluted and fitted with Lorentzian lines to determine the peaks positions (2θ) and the full width at half-maximum values of the peaks. The full width at half-maximum of the peak located at 16.5° and assigned to the (110) reflection of the hydroxybutyrate (HB) crystals[6,10] was used to compute the crystallite size (L). χ_c was computed for each sample from the ratio of the summed area of all of the deconvoluted peaks over the area of the whole spectrum.

Table III. T_g, T_c, T_{m3}, and T_{m4} Measured during the DSC Heating Run Performed on Samples Aged for 1 Week

Sample	T_{g1} (°C)	T_{g2} (°C)	T_{m3} (°C)	T_{m4} (°C)	χ_c (%)	L (nm)
CW 100%	3	46	128	155	26.5 ± 2.4	0.28 ± 0.12
CW 89%	—	52	125	153	25.7 ± 1.9	0.50 ± 0.06
OOMW 100%	−11	53	122	145	28.2 ± 0.7	0.71 ± 0.04
SYNTH 100%	—	49	138	158	26.5 ± 4.2	0.64 ± 0.20
SYNTH 94%	1	66	123	146	27.0 ± 2.7	0.81 ± 0.04

The experimental error for the transition temperatures was 1°C. The χ_c and L values are for samples rimmed from the shearing plates of the rheometer.

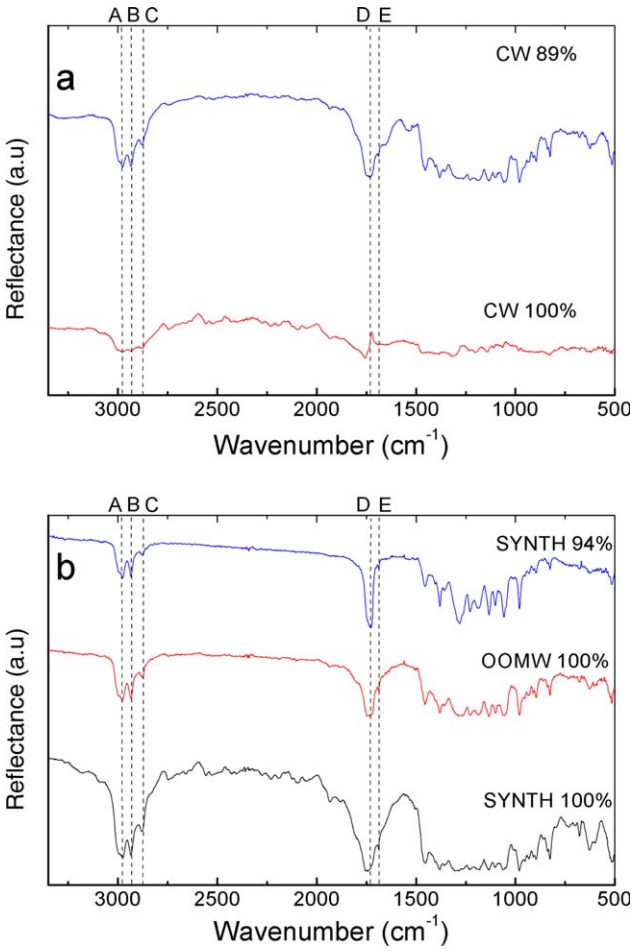

Figure 1. DRIFT spectra of MMC PHA obtained from (a) CW and (b) OOMW or synthetic mixed cultures. The vertical dotted lines indicate the absorbance bands assigned to stretching modes of (A–C) methyl and methylene groups and (D,E) ester groups. See the text for details. [Color figure can be viewed in the online issue, which is available at wileyonlinelibrary.com.]

Rheology

All of the samples in powder form were compression-molded into disks for 3 min at 150°C under 20 tons of pressure. This temperature corresponded to the incomplete melting of the polymers and resulted in the sintering of the powders into a disk. The latter facilitated the fast loading into the parallel plates of a stress-controlled rheometer (ARG2, TA Instruments) and thus ensured a minimal thermal degradation of the MMC PHBVs. Within 4 h after their preparation, the disks were loaded at 150°C, and both the temperature and sample thickness were adjusted within roughly 5 min at $T_{m2} + 5$°C and 1 mm, respectively. This temperature was chosen because it corresponded to the actual melting of the disks, whereas at $T_{m4} + 5$°C, some samples would not melt or would only partially melt (cf. Tables II and III). The excess melt was then quickly rimmed from the parallel plates. The rimmed materials were cooled to room temperature and stored for 1 month for later WAXD analysis. We studied he thermal stability of the melts at $T_{m2} + 5$°C by testing it for 5 min with a small-amplitude oscillatory shear of 1 Hz and a strain of 1% for samples CW 89% and SYNTH 94% and a strain of 5% for all of the remaining samples. Such strain amplitudes were chosen to guarantee that we recorded the sinusoidal stresses while achieving the best torque sensitivity. Then, a frequency sweep from 100 Hz down to 0.01 Hz was performed with small-amplitude oscillatory shear strains of 1 or 5%, as described previously. The flow curves were measured at $T_{m2} + 5$°C with new sample disks, and the experimental protocol described previously for sample loading. Steady-state shear rate sweeps were performed from 0.05 to 10 s^{-1}, and the *steady state* was defined as the shear viscosity variation inferior to 5% for 20 s.

RESULTS

Characterization of the Recovered PHA Residues

The main characteristics of the studied MMC PHBVs are gathered in Table I. Overall, the total amounts of impurities determined by TGA consistently matched the amounts determined by gas chromatography for all of the samples. The analysis of the TGA data at the highest temperatures indicated that inorganic impurities were present in a lesser amount than organic impurities for all of the samples. The small amounts of impurities in samples SYNTH 100%, OOMW 100%, and CW 100% impeded any further insight into the type of residues remaining after purification. In contrast to this, the data in Table I show that the MMC PHBV obtained from CW contained significantly more proteins and sugars than the MMC PHBV obtained from a synthetic mixture of acetic and propionic acid. The composition of ash found in CW 89% was as follows: 49% Ca, 28% Na, and 23% Fe. The contents of Cu, Mg, and K were below the detection limit of ion chromatography. The composition of ash found in SYNTH 94% could not be established because of the small amount of the sample (and thus of ash after incineration) available for analysis. The weight-average molecular weight (M_w) distributions are also reported for all of the samples in Table I. The purification of sample CW 89% essentially gave a more monodisperse polymer, as the apparent change in M_w was balanced by the larger M_w/number-average molecular weight (M_n) of CW 89%. Samples SYNTH 100% and SYNTH 94% showed larger polydispersity indices when compared to other MMC PHBVs. Such large M_w/M_n values are not unusual because MMC PHBVs with M_w/M_n of 7 have been reported elsewhere.[30] The large polydispersity in the molecular mass distribution of the SYNTH samples was related to variations from batch to batch, which resulted in significant deviations in the M_w values of different batches. After accumulation, the PHA-rich biomasses underwent different digestion lengths within the extraction reactor; this likely resulted in significant deviations in M_w, as explained elsewhere.[25] Note that several batches were needed to recover the necessary amount of MMC PHBVs to conduct the thermal and rheological characterizations reported later.

Effect of the Recovered PHA Residues on the Chemical Patterns of the MMC PHBVs

Figure 1 shows that the DRIFT spectra of all of the samples exhibited the diagnostic absorption bands assigned to the following chemical groups[31] and often reported for PHBV and the products of their thermal degradation:[32] symmetric stretching of methyl (band A at 2960 cm^{-1}) and asymmetric stretching of

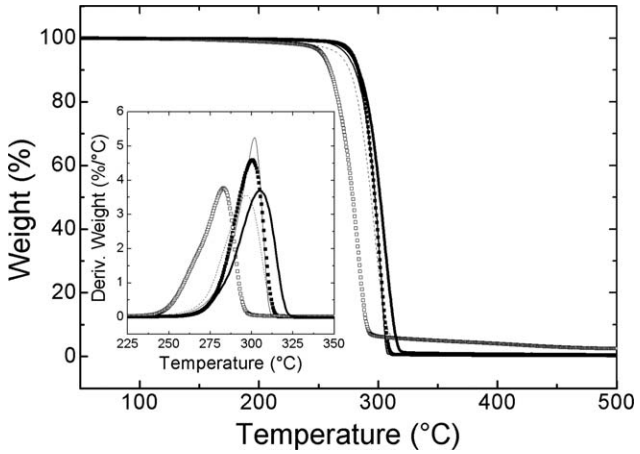

Figure 2. TGA of (■) CW 100%, (□) CW 89%, (—) OOMW 100%, (—) SYNTH 100%, and (- - -) SYNTH 94%. The inset shows the temperature derivatives of the thermal dependence of the sample weights.

methylene (band B at 2930 cm^{-1}), methyl (band C at 2870 cm^{-1}), esters (band D at 1730 cm^{-1}), and esters of 2-butenoic acids (band E at 1690 cm^{-1}). The DRIFT spectra of the PHBVs obtained from CW showed both qualitative and quantitative differences. The DRIFT spectrum of the purified sample did not show the band assigned to esters of the 2-butenoic acids; this suggested that this band mainly had contributions from the residues that were removed during purification. The remaining signals only exhibited quantitative differences; this indicated different compositions in the CH_2 and CH_3 contents of the purified PHBV and PHBV containing 11% residues. The PHBV samples obtained from SYNTH and from OOMW showed qualitatively similar DRIFT spectra, with only slight differences in the relative intensities of the absorption bands. This indicated that the corresponding amounts in impurities ($\leq$6%) were too small to qualitatively affect the band assigned to 2-butenoic acid. In contrast, the recovered PHA residues affected the ratios computed from the intensity of band D over the intensity of band A. Samples SYNTH 100% and OOMW 100% showed similar ratios of 0.85 ± 0.05, whereas a significantly smaller ratio of 0.59 ± 0.05 was computed from the DRIFT spectrum of sample SYNTH 94%. Thus, a relative content in ester groups was computed from the DRIFT data, and this, therefore, indicated at least a minimum amount of 6% recovered PHA residues. Note that such a ratio could not be computed for the CW samples, possibly because of the larger HV and residue contents for these PHBVs. In addition, a ratio including intensities from the bands assigned to 2-butenoic acid could not discriminate between the samples. The FTIR spectra of the MMC PHBVs produced with the same route that we used for samples SYNTH 100% and SYNTH 94% were reported recently.[13] For samples possessing as much as 40 mol % HV, a band was found at 1008 cm^{-1}; this band was assigned to the carbonyls of the HV blocks. This band was only resolved in the DRIFT spectrum of sample CW 89%, which was expected, as this material showed larger amounts of HV and impurities.

Thermal and Semicrystalline Properties

The thermal degradation of all of the PHBV samples is displayed in Figure 2. All of the TGA curves of the samples containing impurities showed a decrease starting at lower temperatures when compared with their purified counterparts. The earlier weight loss confirmed that the presence of large amounts of recovered PHA residues had a negative effect on the thermal stability of these biodegradable polymers.[18] Curves of the purified samples could not be superimposed on the curves of samples containing residues. Part of these residues, such as Ca or Mg ions or oligomers with different end chains, could trigger the thermal degradation of PHBVs at lower temperatures[18,19,33] or could even start to degrade at significantly lower temperatures; this would result in a primary step decrease at earlier temperatures.[20] In addition, other residues degrade at temperatures larger than the ones probed here because, at 500°C, a weight could still be measured. From the latter, the w values in the samples could be computed. These amounts are reported in Table I and compared well with the residues contents evaluated from chemical analysis. Overall, the results from TGA suggest that a small amount of residues remained even after the purification step involving precipitation in iced methanol. The inset in Figure 2 illustrates the maximum of the weight derivative [corresponding to the midpoint of the step decrease of the sample weight with increasing temperature and defined as the degradation temperature (T_d), reported in Table II]. This maximum, and thus its thermal location T_d, was shifted by 17°C for MMC PHBVs made from CW, whereas the shift was reduced to roughly 5°C for the SYNTH samples. In addition, the purified PHBV, still with residual impurities on the order of 1–3 wt %, showed different T_d's.

Figure 3 shows the DSC heating curves of the samples cooled from the melts (run II, as explained in the Experimental section). All samples exhibited a glass transition at temperatures close to 0°C; this was in agreement with reported temperatures for PHBVs with similar HV contents and tested with DSC.[6,30] The MMC PHBV samples containing recovered PHA residues presented a lower T_g. This seemed to be a rather stiff result because the same trend was observed independent of the feedstock. All of the samples presented a crystallization process upon heating; this was related to the previous fast cooling from

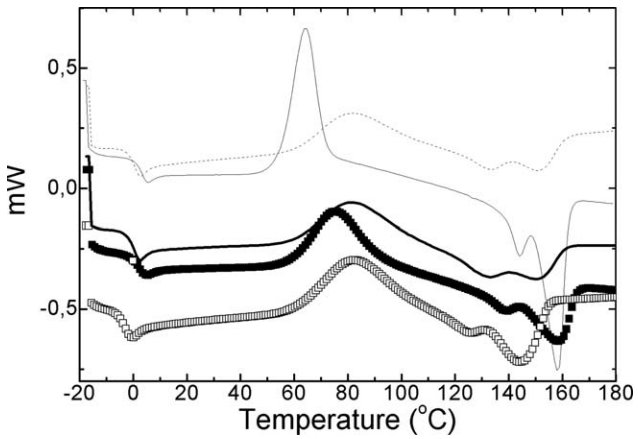

Figure 3. DSC curves recorded during run II for (■) CW 100%, (□) CW 89%, (—) OOMW 100%, (—) SYNTH 100%, and (- - -) SYNTH 94%.

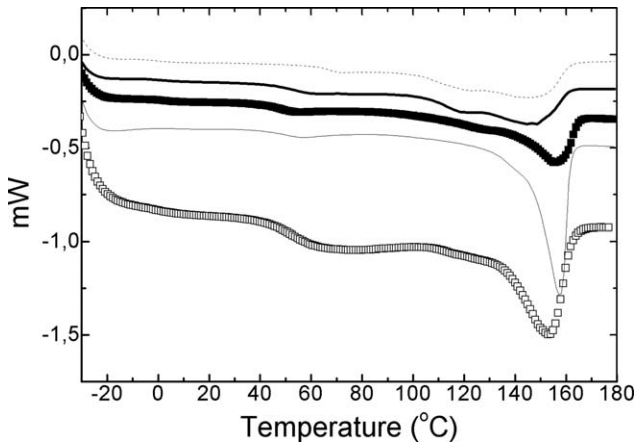

Figure 4. DSC curves of samples aged for 1 week at room temperature after run II for (■) CW 100%, (□) CW 89%, (—) OOMW 100%, (—) SYNTH 100%, and (- - -) SYNTH 94%.

the melt. Two T_m's were observed for each of the samples. The two melting processes originated from the block copolymer structure of the PHBV obtained from the pulse-wise feeding strategy[23–25] because the HV blocks melted before the HB blocks.[6] Note here that similar DSC curves with distinguishable melting processes were reported for immiscible blends of PHB and PHBV[34] and for PHBVs obtained from MMC with similar feeding sequences.[13,35,36] The χ_c values computed from the two melting processes displayed in Figure 3 are reported in Table II. χ_c only serves here as a comparative index of χ_c of the MMC PHBV samples. It does not correspond to the true χ_c of the samples, as this would require the use of the melting enthalpy of a fully crystalline PHBV with corresponding chemical composition in place of the ΔH_0 used in eq. (1).[13,35]

PHBVs are known to exhibit a slow crystallization process. The latter is at the origin of the embrittlement and changes in the barrier properties of PHBV packages.[7] The slow crystallization process is mirrored in the DSC runs performed after 1 week of

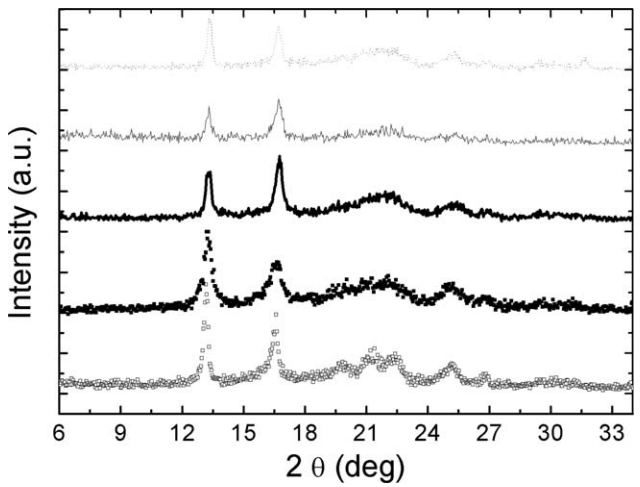

Figure 5. WAXD spectra of the 1-month-old PHBV samples rimmed from the shearing plates of the rheometer at $T_{m2}+5$°C for (■) CW 100%, (□) CW 89%, (—) OOMW 100%, (—) SYNTH 100%, and (- - -) SYNTH 94%.

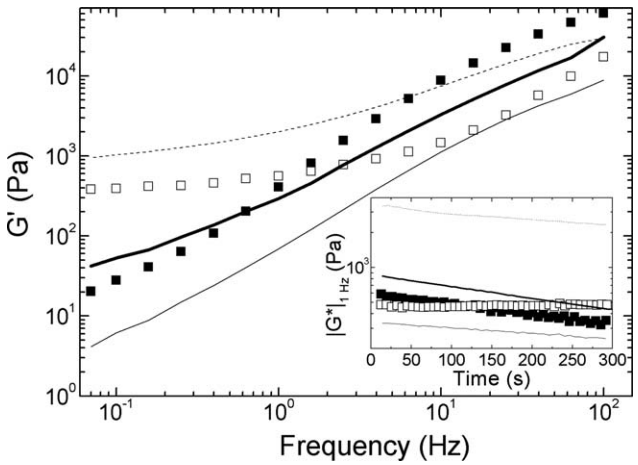

Figure 6. Frequency dependence of the G' values of the MMC PHA samples measured at $T_{m2}+5$°C after the record of a time sweep (inset) performed at the same temperature for (■) CW 100%, (□) CW 89%, (—) OOMW 100%, (—) SYNTH 100%, and (- - -) SYNTH 94%.

aging and displayed in Figure 4. These DSC curves did not show any cold crystallization process. Instead, a glass transition appeared at a higher temperature (T_{g2}); this was, therefore, related to the HB blocks[6] and was added to the glass transition of the HV blocks (T_{g1}). The aging of the polymers also changed their melting behavior, as the peak corresponding to the melting of the HV blocks (occurring at T_{m3}, see Table III) was less resolved when compared to those of the quenched samples.

The semicrystalline characteristics of the aged MMC PBHVs are illustrated in Figure 5. All of the peaks originating from the X-rays diffraction of HB crystals and referenced in the literature[6,10] were resolved in the WAXD spectra displayed in Figure 5. All of the spectra were qualitatively similar; this indicated that the recovered PHA residues did not promote a new crystalline structure. The results from the quantitative analysis of the WAXD spectra are summarized in Table III. χ_c was overall the same for all of the samples; this confirmed that χ_c in the PHBVs did not depend on the chemical composition.[6,37,38] More important, it showed that the residues had no effect on χ_c. However, the crystals were larger when recovered PHA residues were extracted together with the biopolyester, as L is an increasing function of w.

Rheological Properties

Figure 6 presents the rheological characteristics of all of the MMC PHBV samples at a common reference temperature, that is, 5°C above T_{m2}. The rheological assessment of the melt thermal stability for residence times relevant for extrusion, compounding, or injection molding is displayed in the inset in Figure 6, which illustrates the time dependence of the dynamic shear modulus ($|G^*|$). All of the samples except CW 89% showed a drop in the melt elasticity with time. Such a decrease has been widely reported in the literature and is explained by the kinetics of chain scission and the consequent drop in molecular mass at T_m.[39–41] Sample CW 89% showed a nearly constant $|G^*|$ during the 5 min of the test. This steady elasticity indicated that the recovered PHA residues acted as a thermal stabilizer. However, the elastic drop in $|G^*|$ for sample SYNTH 94% nearly

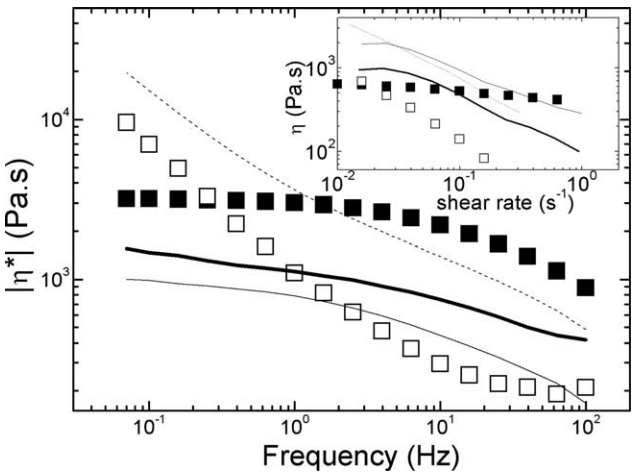

Figure 7. Frequency dependence of $|\eta^*|$ measured at $T_{m2} + 5°C$ for all of the MMC PHAs. The inset shows the flow curves measured at $T_{m2} + 5°C$ for (■) CW 100%, (□) CW 89%, (—) OOMW 100%, (—) SYNTH 100%, and (- - -) SYNTH 94%.

matched the drop of the purified counterpart. This result was in harmony with the thermomechanical degradation of a commercial PHBV.[20] In this study, the commercial PHBV samples were purified and then formulated with separated residues. The time dependence of the torque recorded during the melt mixing showed that the addition of 4 wt % recovered PHA residues did not affect the kinetics of degradation. However, such data could not discriminate between thermal and mechanical degradation. The semilogarithmic plot in the inset in Figure 6 demonstrated that the thermal degradation showed an exponential dependence on time. Accordingly, all of the rheological functions measured during the frequency and shear rate sweeps tests were corrected for thermal degradation, according to an approach proposed elsewhere.[39] The fit of the data in the inset in Figure 6 by an Arrhenius equation allowed us to compensate for the thermally induced decrease in the shear storage modulus (G'), dynamic shear viscosity ($|\eta^*|$), and η. The frequency dependence of G' depicted in Figure 6 shows that residues also had an effect on the viscoelasticity of the MMC PHBVs. Samples with residues were essentially more elastic than the purified samples. In particular, an elastic plateau at lower frequencies showed up when recovered PHA residues were present. This was reminiscent of a reinforcing effect by solid fillers, which percolated in the viscous melt.[42] The similitude with reinforced polymer melts included a vertical shift in G' at larger frequencies when we compared samples SYNTH 100% and SYNTH 94%. However, such behavior was absent in the high-frequency regime of the curve of sample CW 89%. The effect of MMC PHBV purification on the melt viscoelasticity is also illustrated in Figure 7, which shows the frequency dependence of $|\eta^*|$ for all of the samples. The low-frequency regime showed a transition from an elastic-like behavior (characterized by a nearly linear decrease in $|\eta^*|$) to a Newtonian behavior (characterized by a plateau in $|\eta^*|$) that occurred upon the purification of MMC PHBV. Note here that a shift from Newtonian behavior to elastic behavior resulting from the addition of a bacterial biomass containing PHA to a commercial biodegradable plastic has recently been reported.[21] The inset in Figure 7 presents the flow curves measured for all of the samples and also illustrates the benefits of having 6–11 wt % recovered PHA residues in the MMC PHBV melts. As expected from the reinforcement effect detected in Figure 6, samples containing impurities showed stronger shear thinning. This was clearer in the MMC PHBV fermented with CW, as the purified sample exhibited a virtually Newtonian behavior in the range of shear rates tested, whereas the sample with 11 wt % impurities showed a strong shear thinning. However, the data in the inset of Figure 7 did not permit any extrapolation of the MMC PHBV viscoelastic behavior at shear rates relevant for processes such as extrusion. Capillary rheometry is needed for that purpose, but this characterization requires hundreds of grams of polymer, whereas only tens of grams were available for this study.

DISCUSSION

Effects of the Accumulation Methods and HV Content

Samples OOMW 100% and CW 100% were produced by the pulse feeding of the accumulation reactor. Thus, these MMC PHBVs should have exhibited a block copolymer structure with different distributions of HV and HB blocks along the copolymer chain, whereas sample SYNTH 100% should have exhibited a more statistical copolymer configuration. In addition, the three polymers showed different molecular mass distributions. All of these parameters affected the semicrystalline structure and the thermorheological properties of the MMC PHBVs.

The T_g's reported in Table II for the purified samples did not show the expected decrease with increasing HV content[6,35] because the T_g of sample CW 100% was between the T_g's measured for samples CW 100% and SYNTH 100%. The same remark holds true for T_{g1} and T_{g2}. Note, however, that two T_g's were measured during the second heating of the MMC PHBVs produced with the pulse-feed method, in contrast to the single T_{g2} found for sample SYNTH 100%. The presence of two glass transitions was reminiscent of the nanoscopic phase separation in block copolymers of MMC PHBVs.[35] We could not exclude any effect of the molecular mass of the HV or HB blocks on the glass transitions of the corresponding blocks. Thus, any relationship between the HV content and all of the T_g's was hard to predict without a better knowledge of the blocks sizes. The same difficulty arose when we examined the effect of the HV content on the T_m's. For instance, all of the T_m's measured for sample CW 100% were significantly larger than those measured for the MMC PHBVs with similar block copolymer structures but with less HV content (see sample OOMW 100%). However, sample SYNTH 100% showed the highest T_m's. Laycock *et al.*[35] reported that the T_m's of aged samples remained virtually the same, independent of the block copolymer or random copolymer structure and the HV content. However, the frequency of pulses, the feedstocks, and the downstreaming processes used differed from the ones used here. Thus, the copolymer structure of the MMC PHBVs and inherent thermal properties seemed to be very sensitive to the production and recovery methods. Similarly, it has been shown that the temperature of crystallization increased with the HV content and that at constant HV contents, a random copolymer structure gave a higher T_c.[35] The

data in Table II suggest the opposite. However, the inspection of the degree of crystallization of the aged samples suggested that χ_c was not correlated with the HV content nor with the copolymer structure, at least within the range of precision given by the analysis of the WAXD spectra. Interestingly, PHBVs with larger HV contents exhibited smaller crystals (cf. the L values for CW 100%, OOMW 100%, and SYNTH 100%). This result was hard to reconcile with the fact that the HV crystals were larger than the HB crystals.[6] Again, other parameters, such as the molecular mass distribution,[43] may have also affected L, and this could explain why both MMC PHBVs produced from CW showed consistently smaller L values when compared to the SYNTH samples, which possessed larger and broader mass distributions.

The rheological data reported in Figures 6 and 7 suggest that no relationship between the HV content in the MMC PHBVs and the rheological functions could be identified. For instance, samples OOMW 100% and CW 100% showed very similar levels of elasticity in the whole range of frequencies tested (see Figure 6), whereas they exhibited different HV contents. Thus, the HV contents were not at play; this was in agreement with the conclusions from a study with commercial PHBV.[39] Other macromolecular parameters, such as the distribution of the molecular mass, were expected to dominate the rheological properties of the polymer melts. The large polydispersity index of sample SYNTH 100% was responsible for the absence of terminal behavior at lower frequencies, shown in Figure 7, in contrast to the Newtonian plateau exhibited by the dynamic viscosity of sample CW 100%. Therefore, the viscosities values at lower frequencies could not be explained simply in terms of the molecular mass of each sample.

Effects of the Impurities

The shift in T_d to lower temperatures was consistent with the two sets of MMC PHBVs studied here; this confirmed earlier reports on the negative effects of residues on the thermal stability of these biopolyesters.[18,19,33] We note here that the shift in T_d was more important for samples CW 100% and CW 89% than for samples produced from synthetic feedstocks. The chemical analysis of residues reported in Table I suggested that the larger content of residual proteins in the CW samples promoted thermal degradation; this was in agreement with earlier findings.[18] To bypass the possible bias brought about by the potential effect of the chemical composition on T_d, one may compare samples OOMW 100% and SYNTH 100%. These two samples exhibited nearly similar amounts of residual impurities and HV contents. The OOMW 100% sample was slightly more thermally stable. This could be correlated with its larger amount in inorganic content and thus confirmed the trend found previously. The recovered PHA impurities shifted T_g to lower temperatures. Although the shift was small, this was a stiff result because this trend was observed for the two sets of MMC PHBVs studied. Thus impurities have a plasticizing effect on the quenched samples. This effect may have originated from the influence of impurities on the composition of the amorphous and crystalline phases and relative volume fractions. With the decrease in T_g taken as an aging effect, we concluded that macromolecules were confined within a smaller volume. Such confinement could have resulted from the presence of impurities in the amorphous phase. However, it was still not clear whether the impurities migrated more into the amorphous phase than into the crystalline phase during the quench. We thus turned to the cold T_c. T_c shifted by 6°C to larger temperatures for the synthetic samples. This effect was reproduced with PHBVs made from CW, for which T_c shifted by 20°C. Such a higher T_c was related to a more difficult cold crystallization, where impurities were expelled toward the amorphous phase. Thus, the amorphous phase incorporated more impurities and showed a larger volume fraction, which translated into a smaller χ_c. However, the picture was different for aged samples, as T_{g2} consistently shifted to higher temperatures when impurities were present (see Table III). Therefore, the plasticizing effect of the residues was related to their influence on the aging of the MMC PHBVs. In contrast to the fresh samples, the χ_c values of the aged samples were not affected by the presence of impurities. However, the crystals were larger and melted earlier (see L, T_{m3}, and T_{m4} in Table III); this suggested that the crystals were less dense, as they incorporated impurities. The lack of impurities in the amorphous phase of the aged samples reduced the free volume and thus increased the T_{g2} values of MMC PHBVs containing recovered PHA residues.

The effects of the recovered PHA residues on the rheological properties of the MMC PHBV melts are illustrated in Figures 6 and 7, where two sets of samples differing only by the level of purity but showing nearly similar molecular mass distributions are compared. Overall, the data in Figure 6 suggest that recovered PHA residues contributed to the thermal stabilization of the MMC PHBVs. This was more evident for MMC PHBVs obtained from CW, as sample CW 89% melted at a temperature significantly lower than sample CW 100% (see Table II). Therefore, the kinetics of thermal degradation were much slower for CW 89% at the tested temperature. As mentioned earlier, the residues acted as reinforcing fillers in the MMC PHBV melts. Thus, the elasticity of the melts was enhanced. Both the thermal stabilization and enhanced melt elasticity were highly positive, as they should have improved the melt processing of the MMC PHBVs. Indeed, the thermal stabilization allowed for longer processing times or simply limited PHBV degradation during the conversion into products. Currently, commercial PHBVs are essentially used in injection molding, as this process involves very short residence times and requires melts possessing rather small viscosities. The results shown here suggest that recovered PHA residues opened up the route for extrusion-based processes of PHBV into plastic products, as longer processing times were possible, and a sufficient melt strength was achieved to sustain postprocessing processes, such as drawing.

CONCLUSIONS

Replicated results were obtained with two sets of MMC PHBVs produced with different fermentation substrates and accumulation routes and showing different HV contents. These results allowed us to draw the following conclusions about the effects of recovered PHA residues on the biopolyester properties:

- The impurities were at the origin of a decrease in T_d, and organic residues were more detrimental to the thermal stability.
- The χ_c values of the aged samples was not affected by the recovered PHA residues, but the size of crystallites increased during the secondary crystallization, as they incorporated impurities segregated in the amorphous phase during quenching.
- The melting of the MMC PHBVs occurred at lower temperatures when PHA residues were recovered together with the PHBV. Because the melts were obtained at lower temperatures, their thermal stability was critically improved.
- The recovered PHA residues improved the melt viscosity and provided better shear thinning.

The improved melt rheology and thermal stability in the presence of recovered PHA residues suggested that there was an interesting outcome of further characterizing the composition of impurities and systematically testing their quantitative influence on the pure PHBV materials as agents for melt processing enhancement. For that purpose, an interesting strategy will be to add organic or inorganic residues in a controlled manner to a clean MMC PHBVs. From there, it would be of interest to devise ways to more economically retain these impurities during the PHA recovery process. However, future studies aimed at evaluating the potential migration and toxicity of the residues recovered together with the MMC PHBVs will be needed before we consider the use of these materials in packaging applications. Another important message drawn from the comparison between the properties exhibited by samples OOMW 100% and SYNTH 100% is that a PHBV from one production and recovery location showing similar HV content may not be exactly the same as one produced from another location.

ACKNOWLEDGMENTS

This study was performed in the framework of the ECOefficient BIOdegradable Composite Advanced Packaging (EcoBioCAP) project, which was supported by the European Commission through the Seventh Framework for Research and Technological Development (FP7/2011-2015) under grant agreement FP7-265669. The authors acknowledge the additional financial support given by FEDER funds through the Operational Competitiveness Programme (COMPETE), National Funds from the Portuguese Foundation for Science and Technology [Fundação para a Ciência e Tecnologia (FCT)] in the scope of projects PTDC/AGR-ALI/122741/2010 and PEst-C/CTM/LA0025/2011 (Strategic Project—LA 25-2011-2012), and Programa Operacional Regional do Norte (ON.2) through the project "Matepro—Optimizing Materials and Processes" (reference NORTE-07-0124-FEDER-000037 FEDER COMPETE).

REFERENCES

1. Plackett, D.; Siro, I. In Multifunctional and Nanoreinforced Polymers for Food Packaging; Lagaron, J. M., Ed.; Woodhead: Cambridge, MA, **2011**; p 498.
2. Bugnicourt, E.; Cinelli, P.; Lazzeri, A.; Alvarez, V. *Express Polym. Lett.* **2014**, *8*, 791.
3. Reddy, M. M.; Vivekanandhan, S.; Misra, M.; Bhatia, S. K.; Mohanty, A. K. *Prog. Polym. Sci.* **2013**, *38*, 1653.
4. Sanchez-Garcıa, M. D.; Gimenez, E.; Lagaron, J. M. *Carbohydr. Polym.* **2008**, *71*, 235.
5. Ariffin, H.; Nishida, H.; Shirai, Y.; Hassan, M. A. *Polym. Degrad. Stab.* **2008**, *93*, 1433.
6. Doi, Y. Microbial Polyesters; VCH: Weinheim, **1990**; p 125.
7. Tsui, A.; Wright, Z. C.; Frank, C. W. *Annu. Rev. Chem. Biomol. Eng.* **2013**, *4*, 143.
8. El-Hadi, A.; Schnabel, R.; Straube, E.; Muller, G.; Henning, S. *Polym. Test.* **2002**, *21*, 665.
9. Furuhashi, Y.; Imamura, Y.; Jikihara, Y.; Yamane, H. *Polymer* **2004**, *45*, 5703.
10. Wang, X.; Chen, Z.; Chen, X.; Pan, J.; Xu, K. *J. Appl. Polym. Sci.* **2010**, *117*, 838.
11. Boufarguine, M.; Guinault, A.; Miquelard-Guinier, G.; Sollogoub, C. *Macromol. Mater. Eng.* **2013**, *298*, 1065.
12. Pardo-Ibáñez, J.; Lopez-Rubio, A.; Martínez-Sanz, M.; Cabedo, L.; Lagaron, J. M. *J. Appl. Polym. Sci.* **2014**, *131*, 39947.
13. Martínez-Sanz, M.; Villano, M.; Oliveira, C.; Albuquerque, M. G. E.; Majone, M.; Reis, M.; Lopez-Rubio, A.; Lagaron, J. M. *New Biotechnol.* **2014**, *31*, 364.
14. Johnson, K.; Jiang, Y.; Kleerebezem, R.; Muyzer, G.; van Loosdrecht, M. C. *Biomacromolecules* **2009**, *10*, 670.
15. Serafim, L. S.; Lemos, P. C.; Oliveira, R.; Reis, M. A. M. *Biotechnol. Bioeng.* **2004**, *87*, 145.
16. Koller, M.; Niebelschuetz, H.; Braunegg, G. *Eng. Life Sci.* **2013**, *13*, 549.
17. Madkour, M. H.; Heirich, D.; Alghamdi, M. A.; Shabbaj, I. I.; Steinbuchel, A. *Biomacromolecules* **2013**, *14*, 2963.
18. Kopinke, F.-D.; Remmler, M.; Mackenzie, K. *Polym. Degrad. Stab.* **1996**, *52*, 25.
19. Kim, K. J.; Doi, Y.; Abe, H. *Polym. Degrad. Stab.* **2006**, *91*, 769.
20. Hablot, E.; Bordes, P.; Pollet, E.; Avérous, L. *Polym. Degrad. Stab.* **2008**, *93*, 413.
21. Scaffaro, R.; Dintcheva, N. T.; Marino, R.; La Mantia, F. P. *J. Polym. Environ.* **2012**, *20*, 267.
22. Reis, M. A. M.; Albuquerque, M. G. E.; Villano, M.; Majone, M. In Comprehensive Biotechnology, 2nd ed.; Moo-Young, M., Ed.; Elsevier: Amsterdam, **2011**; Vol. *6*, p 669.
23. Duque, A. F.; Oliveira, C. S. S.; Carmo, I. T. D.; Gouveia, A. R.; Pardelha, F.; Ramos, A. M.; Reis, M. A. M. *New Biotechnol.* **2014**, *31*, 276.
24. Campanari, S.; Silva, F. A.; Bertin, L.; Villano, M.; Majone, M. *Int. J. Biol. Macromol.* **2014**, *71*, 34.
25. Villano, M.; Valentino, F.; Barbetta, A.; Martino, L.; Scandola, M.; Majone, M. *New Biotechnol.* **2014**, *31*, 289.
26. Lowry, O. H.; Rosebrough, N. J.; Farr, L. A.; Randall, R. J. *J. Biol. Chem.* **1951**, *193*, 265.
27. Dubois, M.; Gilles, K. A.; Hanilton, J. K.; Rebers, P. A.; Smith, F. *Anal. Chem.* **1956**, *28*, 350.

28. Serafim, L. S.; Lemos, P. C.; Torres, C.; Reis, M. A. M.; Ramos, A. M. *Macromol. Biosci.* **2008**, *8*, 355.

29. Barham, P.; Keller, A. J.; Otun, E. L.; Holmes, P. A. *J. Mater. Sci.* **1984**, *19*, 2781.

30. Montano-Herrera, L.; Pratt, S.; Arcos-Hernandez, M. V.; Halley, P. J.; Lant, P. A.; Werker, A.; Laycock, B. *New Biotechnol.* **2014**, *31*, 357.

31. Stuart, B. H. Infrared Spectroscopy: Fundamentals and Applications; Wiley: Hoboken, NJ, **2004**.

32. Liu, Q. S.; Zhu, M. F.; Wu, W. H.; Qin, Z. Y. *Polym. Degrad. Stab.* **2009**, *94*, 18.

33. Kawalec, M.; Adamus, G.; Kurcok, K.; Kowalczuk, M.; Foltran, I.; Focarete, M. L.; Scandola, M. *Biomacromolecules* **2007**, *8*, 1053.

34. Yoshie, N.; Saito, M.; Inoue, Y. *Polymer* **2004**, *45*, 1903.

35. Laycock, B.; Arcos-Hernandez, M. V.; Langford, A.; Pratt, S.; Werker, A.; Halley, P. J.; Lant, P. A. *New Biotechnol.* **2014**, *31*, 345.

36. Laycock, B.; Arcos-Hernandez, M. V.; Langford, A.; Buchanan, J.; Halley, P. J.; Werker, A.; Lant, P. A.; Pratt, S. *J. Appl. Polym. Sci.* **2014**, *131*, 40836.

37. Bluhm, T. L.; Hamer, G. K.; Marchessault, R. H.; Fyfe, C. A.; Veregin, R. P. *Macromolecules* **1986**, *19*, 2871.

38. Kunioka, M.; Tamaki, A.; Doi, Y. *Macromolecules* **1989**, *22*, 694.

39. Ramkumar, D. H. S.; Bhattacharya, M. *Polym. Eng. Sci.* **1996**, *38*, 1426.

40. Liao, Q.; Noda, I.; Frank, C. W. *Polymer* **2009**, *50*, 6139.

41. Yamaguchi, M.; Arakawa, K. *Eur. Polym. J.* **2006**, *42*, 1479.

42. Larson, R. G. The Structure and Rheology of Complex Fluids; Oxford University Press: Oxford, **1999**; p 309.

43. Luo, S.; Grubb, D. T.; Netravali, A. N. *Polymer* **2002**, *43*, 4159.